

# MODELING OF THE PRIMARY PROTON BEAMLINE OF THE FERMILAB NUMI PROJECT

S. Striganov, IHEP, Protvino, Moscow, Russia  
 S. Childress<sup>†</sup>, S. Drozhdin, N. Grossman, P. Lucas, N. Mokhov,  
 FNAL, Batavia, IL 60510, USA

## Abstract

The 120 GeV primary proton beamline for the NuMI-MINOS [1] experiment at Fermilab will transport one of the most intense high-energy beams ever constructed. In parallel operation with the Collider program, 80% of the intensity capability of the Fermilab Main Injector can be sent to NuMI. Radiation safety pertaining to residual activity, damage of equipment and irradiation of groundwater is a primary concern. A particular challenge is that this beam will be transported to and targeted in a cavern excavated in rock in an aquifer region. A model of the beamline, including transport elements and excavated enclosures, has been built in the radiation simulation program MARS. This model has been used to determine limits for allowable beam loss, and to study effects of instabilities and of various failure types. Some results obtained with this model are presented.

## 1 MARS MODEL SETUP

MARS14 [2] is a Monte Carlo code for simulation of three-dimensional hadronic and electromagnetic cascades, muon and low-energy transport in shielding and in accelerator and detector components in the energy range from a fraction of an electron-volt up to 100 TeV.

The MARS NuMI beam line description includes technical components (magnets, profile monitors, loss monitors) and beam enclosure profiles. NuMI primary beam transport includes an extraction enclosure at the MI-60 location, a steep angled carrier tunnel through the glacial till and initial dolomitic rock region, and a pre-target tunnel which puts the beam on final trajectory toward the far detector in Soudan, Minnesota.

The beam system includes a total of 45 magnets, of eight different types. An elevation view of part of the transport tunnel is shown in Figure 1.

## 2 CALCULATION PROCESS

The MARS model of the NuMI beam-line was used to calculate beam loss, “star” density, component residual activity and energy deposition in beam loss monitors for a range of operational conditions. These include variations in beam emittance, momentum spread, extraction orbit

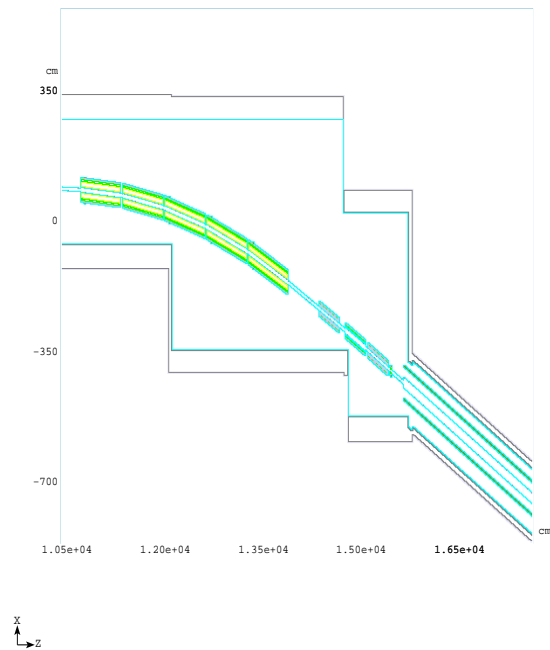


Figure 1: Elevation view of downstream region of extraction enclosure, as the beam is bent downward.

conditions and power supply current. A “star” is defined as a strong interaction vertex with at least one secondary particle having kinetic energy > 50 MeV. The effects of fault mode conditions were also modeled.

Average star densities in the tunnel surround were calculated for a total of seven separate regions, with different tunnel footprints and exterior water flow conditions. These regions, beginning at the downstream end of the extraction enclosure, are shown in Figure 2.

For simulation of energy deposition in beam loss monitors and residual activity determination, default MARS14 thresholds are used (0.2 MeV for muons, charged hadrons, electrons and gammas and  $10^{-9}$  MeV for neutrons).

<sup>†</sup>childress@fnal.gov

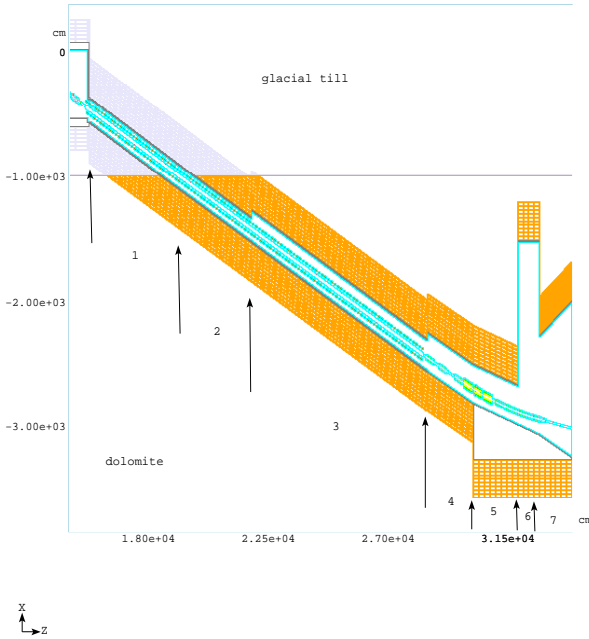


Figure 2: Elevation view of tunnel surround regions for star density evaluation.

### 3 MODEL RESULTS

#### 3.1 Effect of Beam Phase Space and $\delta p/p$

The impact of beam phase space on the cleanliness of NuMI primary beam transport is considered, initially for normal tune conditions. The nominal phase space considered is  $15\pi$  mm-mrad 95% emittance with a  $40\pi$  cut on beam tails. Emittance values are normalized to beam energy of 120 GeV. This cut on beam tails is expected by clipping of tails at low field in the Main Injector, with a  $40\pi$  dynamic aperture through the acceleration cycle.

Beams of different emittance, from  $15\pi$  to  $60\pi$  are transported through the NuMI primary magnet system to determine beam loss fractions at restrictive apertures, and total beam loss. For different emittance beams, the effect of beam tails is considered by determining beam loss both with and without beam tail cuts prior to transport through the NuMI beam-line. Additionally, the effects of  $\delta p/p$  ratios from  $1 \cdot 10^{-4}$  to  $4 \cdot 10^{-4}$  are considered. For each run, a total of 100,000 particles is transported, giving beam loss sensitivity of  $1 \cdot 10^{-5}$ .

At the level of sensitivity considered, no beam loss is seen for  $15\pi$  beam and  $\delta p/p$  ratio of  $1 \cdot 10^{-4}$ . These are considered as representative favorable beam conditions for NuMI, with the small momentum spread achieved by RF manipulations at the extraction energy.

For much larger beam of  $40\pi$  emittance and  $\delta p/p$  ratio of  $2 \cdot 10^{-4}$ , no beam loss is seen when a  $40\pi$  cut on beam tails is imposed. However, without this cut and a

Gaussian beam tail distribution, a total beam loss fraction of  $3.9 \cdot 10^{-4}$  is seen, with similar loss components at several apertures.

#### 3.2 Beam Loss vs. Magnet Current Variations

An important consideration in operational control of beam loss is variation of beam positions due to stability of the Main Injector beam prior to extraction for NuMI, and to NuMI power supply current variations. For this study, a 95% emittance of  $15\pi$  is considered, with beam tails cut off at  $40\pi$  and  $\delta p/p$  ratio of  $1 \cdot 10^{-4}$ .

Beam loss thresholds vs. magnet current variation are determined for each NuMI dipole string supply. An example is shown in Figure 3 for the major down-bend V105, showing the development of beam loss on downstream apertures. As is seen, current instability for this supply should be  $< 0.1\%$  to preclude beam loss, assuming all other conditions are nominal. More stringent constraints can be seen with effects of combined variations in several power supplies.

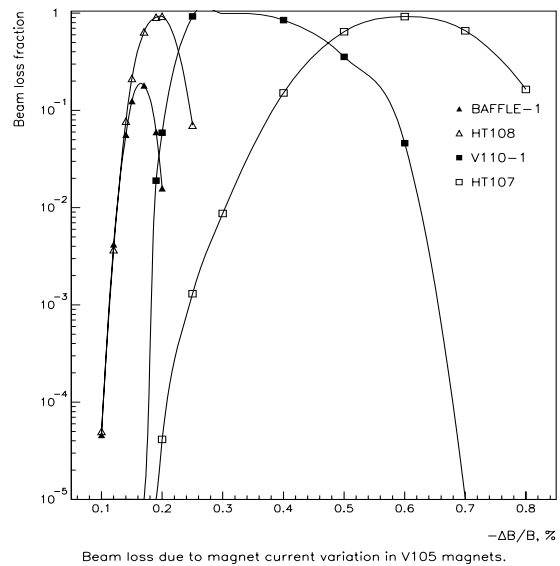


Figure 3: Development of beam loss due to magnet current variations in V105 magnet string.

Combining the effects seen in this modeling with constraints on stability of beam targeting, control of dipole power supply instability is needed between 100 and 400 parts per million, dependent on the strength and location of each set of magnets.

### 3.3 Star Density vs. Beam Loss Modes

From the beam loss studies vs. magnet current variations, 14 different scenarios are identified for detailed modeling of star density. These provide a comprehensive mapping of potential beam loss patterns. An example of star density distributions and energy deposition density in beam loss detectors is shown in Figure 4. Seen are beam loss peaks on either side of the carrier tunnel region, with reduced loss in the most sensitive region for groundwater protection. Average star densities are calculated in the rock surround for a volume containing 99.9% of the total calculated stars for each tunnel region. A separate groundwater model calculation is then done to determine allowable maximum star density for each tunnel region.

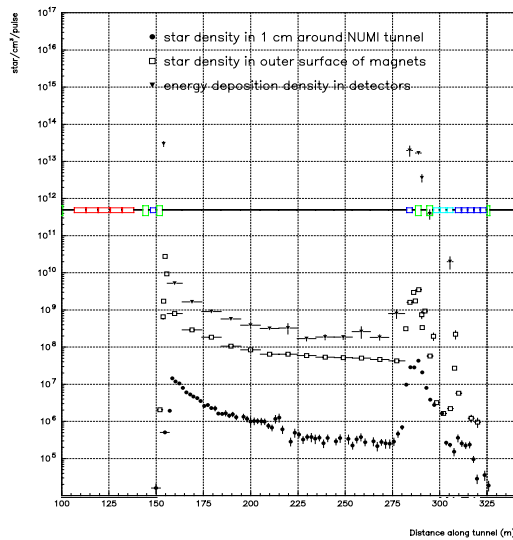


Figure 4: Star density distribution and energy deposition in beam loss monitors for magnet current variation of 0.4% in V105.

Combined calculation results indicate upper limits for average beam loss fraction on transport magnets from  $1.8 \cdot 10^{-4}$  to  $6 \cdot 10^{-3}$  of the high-intensity primary beam flux, dependent on tunnel location. A more severe loss fraction limit of  $10^{-6}$  of the beam is seen in regions of the carrier tunnel. However, in this region geometry constraints preclude direct primary beam loss except for fault modes such as a vacuum pipe collapse or a magnet coil failure.

### 3.4 Beam Loss Correlation

An important consideration in demonstrating capability to understand groundwater activation in protected rock regions is by study of consistency of the star density determination in the rock vs. energy deposition in beam loss monitors for a wide range of beam loss conditions.

This correlation has been studied for different transport regions susceptible to beam loss for a broad range of fractional loss, with consistent results for the ratio of star density vs. loss monitor response.

## 4 SUMMARY

MARS study of NuMI primary beam loss has provided a series of essential results for beam system design. These include:

- Matching of transport element apertures to expectations for beam emittance and momentum spread.
- Determination of current variation limits for major power supplies.
- Specifications of stringent beam loss limits, which must be maintained during beam operation, to provide protection of the groundwater resource.
- Correlation between star density in the tunnel surround with direct observables of loss monitor response and component residual activity.

A comprehensive beam extraction permit system is being designed to closely monitor preceding pulse beam loss conditions and each pulse power supply currents prior to enabling beam extraction for NuMI. Setup of this system is greatly enhanced by results of this beam loss study.

## 5 REFERENCES

- [1] <http://www-numi.fnal.gov:8875/>
- [2] N.V. Mokhov, "The MARS Code System User's Guide", Fermilab-FN-628 (1995); N.V.Mokhov and O.E.Krivosheev, "MARS Code Status", Fermilab-Conf-00/181 (2000); <http://www-ap.fnal.gov/MARS/>